ROYAL SOCIETY OPEN SCIENCE

Research

Check for updates

Author for correspondence:
Benny Borremans
e-mail: bennyborremans@gmail.com

THE ROYAL SOCIETY PUBLISHING

The shape of the contact–density function matters when modelling parasite transmission in fluctuating populations

Benny Borremans[1,4,5], Jonas Reijniers[1,2], Niel Hens[3,5] and Herwig Leirs[1]

[1]Evolutionary Ecology Group, [2]Department of Engineering Management, and [3]Centre for Health Economics Research & Modelling Infectious Diseases (CHERMID–VAXINFECTIO), University of Antwerp, Antwerp, Belgium
[4]Department of Ecology and Evolutionary Biology, University of California Los Angeles, Los Angeles, CA, USA
[5]Interuniversity Institute for Biostatistics and Statistical Bioinformatics (I-BIOSTAT), Hasselt University, Diepenbeek, Belgium

BB, 0000-0002-7779-4107

Models of disease transmission in a population with changing densities must assume a relation between infectious contacts and density. Typically, a choice is made between a constant (frequency-dependence) and a linear (density-dependence) contact–density function, but it is becoming increasingly clear that intermediate, nonlinear functions are more realistic. It is currently not clear, however, what the exact consequences would be of different contact–density functions in fluctuating populations. By combining field data on rodent host (*Mastomys natalensis*) demography, experimentally derived contact–density data, and laboratory and field data on Morogoro virus infection dynamics, we explored the effects of different contact–density function shapes on transmission dynamics and invasion/persistence. While invasion and persistence were clearly affected by the shape of the function, the effects on outbreak characteristics such as infection prevalence and seroprevalence were less obvious. This means that it may be difficult to distinguish between the different shapes based on how well models fit to real data. The shape of the transmission–density function should therefore be chosen with care, and is ideally based on existing information such as a previously quantified contact– or transmission–density relationship or the underlying biology of the host species in relation to the infectious agent.

1. Introduction

The transmission of infections can be sensitive to changes in population density, especially in the case of fluctuating wildlife populations [1–3]. When modelling disease transmission, the probability of encountering an infected individual is typically assumed to be either independent of (frequency-dependent) or linearly dependent on (density-dependent) population density [4]. Sexually transmitted infections are generally described using frequency-dependent transmission because the number of sexual contacts is assumed to remain constant, regardless of population density [5]. Infections that are transmitted through regular 'every-day' contacts are often assumed to be density-dependent [6].

The choice of which contact–density function to use in a model of disease transmission entails potentially significant consequences [7]. Most importantly, the two functions differ in whether or not an infection is expected to persist below a critical density of individuals [8]. The basic reproductive number (R_0), defined as the number of secondary infections arising from the introduction of one infectious individual into a completely susceptible population, is a central epidemiological measure that characterizes the spread of an infection, and provides an immediate approximation as to how rapidly an infection can spread [9]. In its simplest form, $R_0 = \beta N$, where N is the population size and β is the transmission coefficient that consists of the rate p of becoming infected through contact with an infectious individual, multiplied by the contact–density function that equals cN/A (where A is area) when linear (density-dependent) and c when constant (frequency-dependent), and random homogeneous mixing is assumed [10]. When transmission coefficient β changes with density, theory predicts a density below which the transmission rate is too low, causing R_0 to fall below 1 and the disease to disappear, whereas no persistence threshold density exists when β remains constant, independent of density [1,11,12]. Because changes in the transmission coefficient determine how quickly an infection can spread through a population, it can also be expected that the two contact–density functions will differently affect outbreak characteristics such as incidence, prevalence and outbreak size [13].

Because human populations are usually large and stable, and because some types of contacts do not appear to change with population density [14], many models of human disease transmission will not be significantly affected by the choice of the contact–density function. But when one is interested in modelling infection dynamics in populations of different sizes or periodically fluctuating densities, the shape of the assumed contact–density function may become highly important [3]. It is therefore not surprising that studies on how transmission rates and contacts relate to density have mainly been conducted in wildlife [10,15–19]. The main approach in these studies has been to measure disease prevalence in a field or experimental setting in which densities are manipulated or vary naturally, followed by fitting models with different transmission–density functions to the data.

There has traditionally existed a focus on whether transmission is frequency- or density-dependent, and rarely are other, nonlinear transmission–density functions investigated [20,21]. Nevertheless, it has been well established that the binary distinction between density independence and linearity can be inadequate, and a range of other possible nonlinear transmission functions has been suggested, often in the power law, asymptotic or logistic family [10,22–25]. Cowpox virus dynamics in a natural population of field voles (*Microtus agrestis*), for example, has been shown to be best described by a nonlinear power function intermediate between density independence and linearity [15]. Intermediate density-dependence was also observed in *Ambystoma tigrinum* virus transmission in the tiger salamander [22].

Here, we want to investigate whether, and in which situations, implementation of the exact shape of the transmission response function is important. Although it would be possible to mathematically model the effects of different transmission–density functions for any hypothetical combination of demographic pattern and contact–density function, the sheer number of possible functions for each demographic situation would make it almost impossible to decide which functions are biologically relevant. To inform such models in a meaningful way, we need biological background data, i.e. a species for which population dynamics, a contact–density or transmission–density function, and disease dynamics have been quantified, but until recently no such data were available. Using a combination of data from recent experiments in which we quantified contact rates across a wide range of population densities in the rodent *Mastomys natalensis* [26] and the infection parameters of Morogoro virus (MORV) in this rodent [27], we tested the effect of different transmission functions using a simple SIR (susceptible, infectious, recovered) transmission model in annually fluctuating host populations. By implementing a range of hypothetical combinations of infectious period, transmission rate and population size, we assessed what the effects of the contact–density function would be for infections with different characteristics.

2. Material and methods

2.1. Background data

Natal multimammate mice (*M. natalensis*) occur throughout sub-Saharan Africa, and are an important agricultural pest species and natural reservoir hosts for several microparasites that cause disease in humans, including *Yersinia pestis* (bubonic plague), leptospirosis and several arenaviruses including Lassa virus, which can cause severe haemorrhagic fever in humans [28–32]. Multimammate mouse demography has been studied thoroughly, which allows us to create a simple but accurate demographic model that will serve as a basis for transmission modelling (see below). In Tanzania, where most of the studies on its population ecology have been conducted, *M. natalensis* exhibits strong annual population fluctuations, with densities ranging from $10\,\mathrm{ha}^{-1}$ in the breeding season to greater than $300\,\mathrm{ha}^{-1}$ outside the breeding season [33,34]. Importantly, we have recently quantified a contact–density relationship for this species, which provides us with a realistic biological background for fitting the transmission functions [26].

The simulated infection dynamics in this study are based on those of MORV, which naturally occurs in *M. natalensis* in Tanzania, and of which the transmission ecology [35] and patterns of infectivity [27,36] have been documented in detail; it has a latent period of about 3 days between infection and excretion (which we here ignored for simplicity), an infectious period of 30–40 days, and presumably lifelong immunity. MORV transmission can therefore be modelled using a simple SIR model (described below).

2.2. Study design: models

We investigated the effect of four different contact–density functions using stochastic MORV transmission models. While transmission in these models is stochastic, demography was implemented deterministically because this allows us to focus entirely on the effects of stochasticity in transmission, and because it reduces computation time.

2.3. Demographic model

The seasonally fluctuating densities of *M. natalensis* were modelled using a seasonal birth-pulse function, $B(t) = k \exp[-s \cos^2(\pi t - \varphi)]$, as described in Peel *et al.* [37]. This is a flexible function in which a synchrony parameter (s) determines the length of the birth period, and another parameter (φ) determines the timing of the birth period. Parameter k ensures that the annual population size remains the same, by compensating the number of births for the (constant) mortality rate μ [37]. Note that this means that while the *annual* population size is constant, population densities do fluctuate *seasonally* because all births happen within a few months, whereas deaths happen throughout the year. Function parameters were fitted visually to a 20-year dataset of monthly population densities of *M. natalensis* in Tanzania ([33,34] and more recent unpublished data (H Leirs, up to 2017); electronic supplementary material, figure S1–1). This deterministic demography was used as a basis for modelling demography in the stochastic SIR model (described below) in order to avoid the influence of stochastic changes in population density, and because this reduces the number of simulations that need to be performed.

2.4. Transmission model

A standard SIR (susceptible, infectious, recovered) model was used to simulate MORV transmission [38,39], described by the following set of coupled ordinary differential equations:

$$\frac{\mathrm{d}S}{\mathrm{d}t} = B(t)\,N - \beta S \frac{I}{N} - \mu\,S,$$

$$\frac{\mathrm{d}I}{\mathrm{d}t} = \beta S \frac{I}{N} - \gamma\,I - \mu\,I$$

and

$$\frac{\mathrm{d}R}{\mathrm{d}t} = \gamma\,I - \mu\,R,$$

where $B(t)$ is the time-dependent birth function described earlier, μ is the mortality rate, γ is the 1/infectious period and $\beta = cp$ is the transmission coefficient, which consists of p (rate at which S becomes I when in contact with an I individual) and contact–density function $c = f(N/A)$ that can acquire different shapes depending on population density (explained below).

In order to compare invasion and persistence probabilities between different contact–density functions, we used a stochastic discrete time version of this SIR model, where the transition rates between categories were modelled stochastically, resulting in two possible stochastic events: infection (decrease of S, increase of I) and recovery (decrease of I, increase of R). Events were assumed to occur continuously in time at a certain rate, and were modelled using the 'adaptive tau-leap' algorithm described in [37,40]. Briefly, each short time-step δt, the number of events of each type (infection or recovery) that occurs is randomly drawn from a Poisson distribution with mean $r_i \delta t$, where r_i is the rate of each type of event i. If the number of simulated events would cause any of the categories (S, I or R) to fall below 0, δt is halved and new events are drawn (='adaptive tau-leap').

The model started at $t = 0$ and one infected individual was introduced after 1 year, at $t_0 = 1$ ($I \rightarrow 1$) in order to allow the initial population dynamics to stabilize. This infected individual was considered to be at the start of the infectious period upon introduction. Prior to performing the main analyses, the effect of introduction time was analysed. Different introduction times had an effect only on the linear and sigmoid functions, where they resulted in lower invasion probabilities between t_0 values of 1.2 and 1.4, which was probably a result of the low population densities (electronic supplementary material, figure S2–1). There was no effect of introduction time on disease persistence (electronic supplementary material, figure S2–2).

2.5. Four different contact–density functions

The core of this study is the implementation of four different, biologically relevant contact–density functions $c = f(N/A)$ (figure 1):

(a) Constant function (or 'frequency-dependence') $c = a_1 (N/A)^0$, with fitting parameter a_1. This function is independent of density, and typically (but not only, e.g. vector-borne infections [41]) used in the case of sexually transmitted infections where the number of sexual contacts is not expected to change with population density [5,8].

(b) Linear function (or 'density-dependence') $c = a_2 (N/A)$, with fitting parameter a_2. A linear function is typically used when assuming random mixing where (infectious) contacts increase linearly with population density [39,42].

(c) Power function $c = a_3 (N/A)^{0.5}$, with fitting parameter a_3. This function has been used as an 'intermediate' between frequency- and density-dependence [10,22]. A power of 0.5 was used in order to get the intermediate saturating shape, which was the most informative shape for the simulations. The power function contact rates increase at low densities, while the slope decreases at higher densities towards an asymptotic limit. This shape has been observed for contact rates in brushtail possums and elk [43–45], and has been shown to be a better predictor of cowpox transmission patterns than frequency- or density-dependence [15].

(d) Sigmoid function $c = a_5 / (1 + e^{a_6 ((N/A) - a_7)})$ with fitting parameters a_5, a_6 and a_7. This function has a minimum, constant number of contacts at low densities, after which contact rates increase with density until reaching a plateau when reaching a maximum number of contacts. This shape has been observed for multimammate mice contacts [26], and has been proposed previously as a biologically plausible function [10].

These four different functions could, in theory, acquire an infinite number of shapes, so in order to realistically model them they were fitted to empirical contact–density data of *M. natalensis* [26,46] using maximum likelihood.

2.6. Fitting transmission coefficient β

Considering that $\beta = cp$, after fitting contact parameter $c(N/A)$ to contact–density data for the four functions, a transmission rate p had to be determined before being able to compare the effect of the different transmission–density functions. This is exactly equivalent to the situation in which real data are known, but the underlying transmission–density function is not. In such a situation, different transmission–density functions are implemented in a model and fitted to the data. For each contact function c, a different transmission rate p must be fit in order for the transmission–density function to match the real data as closely as possible. If instead we were to use the same transmission rate p for each function, we would, in fact, be comparing entirely different transmission dynamics. Fitting p is typically done using a certain important characteristic of the real data, such as average outbreak
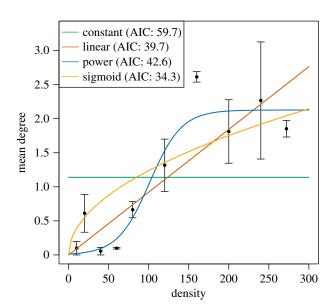
Figure 1. Contact–density functions fitted to experimental data from Borremans *et al.* [26], showing mean degree (the number of individuals one focus individual contacted) for a range of population densities (number of animals per ha = N/A).

size or annual cumulative incidence. For this purpose, we implemented a function-specific constant (q_i) that was fitted for each function i to a common characteristic. Out of numerous possible transmission dynamic characteristics to choose for fitting, we opted for one that ensured that β, summed across the probability distribution of population densities occurring during 1 year in a simulated, deterministic model of demography, was the same for each contact function. Formally, this meant that: $\beta = q_i \times \Sigma_{j=1}^{300} f_c(N/A)_j \times h(N/A)_j$, where f_c is the contact–density function, j is the population density and h is the frequency distribution of densities in a year. We chose this method because it has the advantage of not selecting for certain outbreak characteristics such as prevalence or outbreak size. We nevertheless also examined the effect of using two alternative fitting methods. The first alternative method fits q_i so that a deterministic transmission model resulted in a maximum annual prevalence of 40%. The second alternative method fits q_i so that the final annual number of infections was $2N_0$, i.e. twice (an arbitrarily chosen number) the initial number of individuals. While these alternative fitting methods resulted in highly different values for the constant (density-independent) function, the three other functions were always very similar (electronic supplementary material, table S3–1 and figure S3–1). As we are mainly interested in the differences between the three non-constant functions, we did not further investigate the effects of these alternative β-fitting methods.

2.7. Statistics

The effects of the contact–density functions were investigated through a number of meaningful epidemiological parameters: (i) SIR dynamics, including prevalence (I/N); (ii) invasion probability, defined as the proportion of stochastic simulations in which the infection manages to survive the first year after introduction, conditional on having started successfully (successful start = infection persistence time $> t_0 +$ infectious period). This definition was chosen for simplicity, biological relevance and consistency with a previous model of MORV transmission [19]; and (iii) persistence probability, defined as the proportion of simulations in which the infection is still present at $t = 10$ years, conditional on having survived the first year.

Invasion and persistence were estimated under a number of conditions of population size (N_0), infectious period ($1/\gamma$) and transmission rate (p), where for each combination of conditions 1000 simulations were run. While we modelled changes in population *density* for each combination of parameters, we also assessed the effect of population *size* because this is expected to affect the probability for the infection to disappear from the population, independent of density. In order to ensure that we here implemented the effects of population size and not density, population density N/A was calculated assuming that the area occupied when initial population size $N_0 = 100$ is 1 ha, and that area increases linearly with increasing values of N_0 (i.e. when initial population size increases, area also increases).

This, for example, means that while population *density* fluctuates seasonally in exactly the same way for $N_0 = 100$ and $N_0 = 1000$ (or any other N_0), the former assumes an occupied area of 1 ha and the latter an area of 10 ha. Because transmission events are stochastic, the size of the occupied area can have important consequences for virus invasion and persistence.

Tested infectious periods: 1, 7, 14, 30, 60 and 120 days. Tested transmission rates: 1, 5, 10, 25, 50, 75, 100 and 125. Tested population sizes: 100, 500, 1000, 5000, 10 000, 50 000 and 100 000.

3. Results

3.1. Contact–density function fit to data

The four fitted contact–density functions were: $c = 1.14(N/A)^0$ (constant), $c = 0.0092(N/A)$ (linear), $c = 0.124(N/A)^{0.5}$ (power), $c = 2.13/(1 + e^{-0.05\,((N/A)-101.2)})$ (sigmoid). As shown in figure 1, a sigmoid contact–density function resulted in the best fit to contact–density data measured for *M. natalensis* in a previous field experiment [26], while the constant function clearly did not fit the data well. AIC values for the functions were 59.7 (constant), 39.7 (linear), 42.6 (power), 34.3 (sigmoid). Akaike weights were 0.00 (constant), 0.06 (linear), 0.01 (power), 0.92 (sigmoid), providing additional support for the much better fit of the sigmoid function.

3.2. SIR dynamics and prevalence

Because we are interested in the qualitative effects of the contact–density functions rather than in detailed differences that are specific to the model system, we here report the results with a focus on the qualitative aspects of SIR dynamics and prevalence. The constant function resulted in a relatively low epidemic peak during the breeding season, while the other three functions showed a clear epidemic peak where prevalence (proportion Infecteds; figure 2, red curves) increased sharply for the linear and sigmoid functions, but more gradually for the power function. Median peak prevalence for the four functions: 45% (constant), 68% (linear), 60% (power) and 72% (sigmoid). The dynamics of the proportion of Recovered (immune–antibody-positive; figure 2, blue curves) individuals were highly similar for the four functions, although they did differ in how low the Recovered proportion becomes at the end of the birth pulse: 15% (constant), 2% (linear), 14% (power) and 0.5% (sigmoid). There was a steeper build-up of Susceptibles (figure 2, green curves) for the linear and sigmoid than for the other two functions, due to the fact that transmission rates started increasing later in the year (at higher densities).

3.3. Invasion and persistence

Invasion and persistence probabilities were investigated for a range of population sizes (N_0), infectious periods ($1/\gamma$) and transmission probabilities (p). Note that while infectious period results are reported in absolute days, they can also be interpreted in relation to the demographic timescale used in the simulations (e.g. annual breeding, brief recruitment period), which will aid comparison with other pathogen–host systems in which host densities fluctuate [37].

Successful invasion and persistence were more often observed for the constant function than for the other functions (figures 3 and 4). Even at low population sizes, successful invasion was almost certain for infectious periods of 30 days and longer, and was even observed for an infectious period of 7 days in sufficiently large populations. By contrast, for the other functions, successful invasion was never observed below infectious periods of 7 days, and even with an infectious period of 30 days invasion was rare for the sigmoid function. For the linear function, invasion probabilities were lower than for the power function, whereas persistence probabilities for these two functions were similar. The sigmoid function resulted in the lowest invasion or persistence success, where persistence was rarely observed for an infectious period of 30 days. Even when the infectious period was 60 days, persistence was observed only when population size was sufficiently large (e.g. 50% for a population size of 5000).

The effect of transmission rate on invasion and persistence was similar between the constant, linear and power functions, although the constant function still resulted in more successful invasion/persistence at lower transmission probabilities (electronic supplementary material, figures S4–1 and S4–2). The sigmoid function, however, was more affected by transmission probability than the other three functions, where persistence was only possible for a combination of high transmission rate and large population size (electronic supplementary material, figure S4–2).
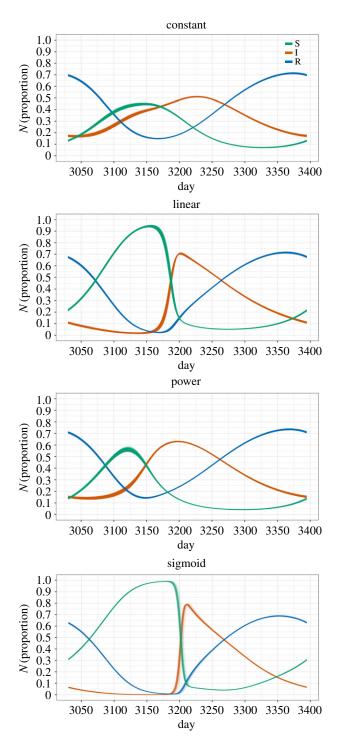
Figure 2. SIR dynamics for the four different contact–density functions. For each simulation run in which there was successful persistence, the 8th year was retained (days 3030 to 3395). The figure shows all these outputs plotted on top of each other. The increase in Susceptibles corresponds with the birth pulse. Infectious period $1/\gamma = 60$ days, transmission rate $p = 50$, initial population size $N_0 = 100\,000$.

4. Discussion

Population densities often vary in space or time, and this can influence parasite transmission. Using data-driven models of virus transmission in a fluctuating population, we found that the way in which the transmission–density function is modelled can have important consequences for estimating invasion and persistence success.
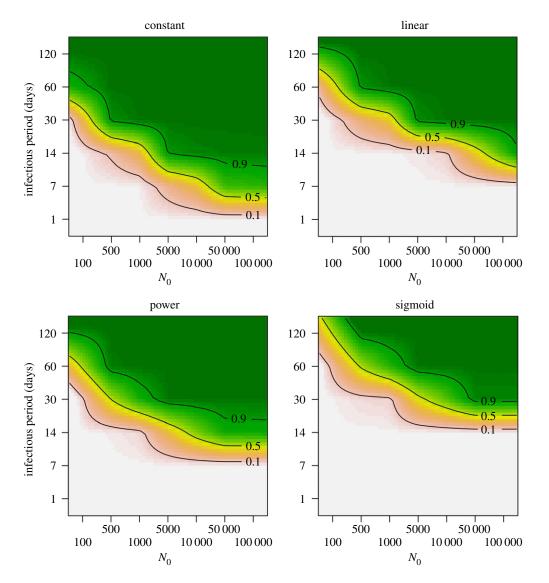
Figure 3. Invasion probabilities for the different contact–density functions, for a range of infectious periods $1/\gamma$ and initial population sizes N_0 (transmission rate $p = 50$). Simulations were conducted for all values indicated by tick marks on the axes, and results are interpolated between these values for illustration.

While SIR dynamic patterns for the constant function were distinct from those of the three density-dependent functions, these three functions did not result in highly different SIR dynamics. Infection prevalence (the proportion of Infecteds) and seroprevalence (the proportion of Recovereds) patterns were very similar for the linear and sigmoid functions. For the power function, seroprevalence and infection prevalence patterns were slightly smoother, with less pronounced peaks, than for the linear and sigmoid functions. Invasion and persistence were clearly affected by the shape of the transmission–density function. They were always higher for the constant function than for the other functions. The sigmoid function resulted in the lowest invasion and persistence probabilities, and was most sensitive to population size, length of the infectious period and transmission rate. Invasion and persistence success for the linear and power functions were intermediate between the constant and sigmoid functions. Depending on the time at which the infection is introduced, the differences in invasion and persistence probability between the contact functions can become even more pronounced.

The different consequences of the contact–density functions can probably be attributed to a number of key differences in their shapes. Considering that the infection is most sensitive to extinction during periods of low population density, the size of transmission coefficient β at low densities will be a highly influential factor. An important consequence of this is that larger population sizes are necessary for successful disease invasion/persistence when β is low during low-density periods. In our case, for example, a minimum population size of 10 000 (equivalent to a 100 ha area) was necessary for a 50%
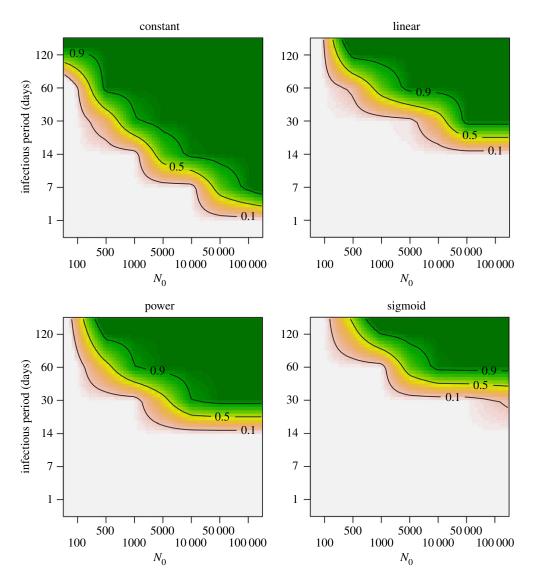
Figure 4. Persistence probabilities for the different contact–density functions, for a range of infectious periods $1/\gamma$ and initial population sizes N_0 (transmission rate $p = 50$). Persistence probabilities were calculated using only simulation runs in which there was successful invasion. Simulations were conducted for all values indicated by tick marks on the axes, and results are interpolated between these values for illustration.

persistence success rate for the power function (30-day infectious period), while this was 50 000 for the linear function and larger than 100 000 (not tested) for the sigmoid function. Knowledge of contact rates at low population densities is therefore critical when estimating invasion and persistence thresholds. A second important factor is the rate at which β increases with density. The epidemic peak will be more pronounced when there is a strong increase of β with density (e.g. the sigmoid function at intermediate densities, but also the linear and power functions). The sigmoid function, for example, results in a steep increase in transmission rates during the juvenile recruitment season as soon as a threshold density of Susceptibles is reached (here around 80–100 ha^{-1}).

When considering both the SIR dynamics and invasion/persistence of the three density-dependent functions, a contrast emerges than can have significant implications for fitting a β-density function to epidemiological data: while there was a clear effect of function shape on invasion and persistence, SIR dynamic patterns were less distinct. This means that it could be difficult to discern between different contact–density functions when fitting model parameters to real, inherently noisy data [3,10,15]. Nevertheless, because the functions do introduce different invasion and persistence probabilities, it will, in some situations, be crucial to implement the correct function. Ideally, this choice is based on the quantified contact–density or transmission–density relationship of the host/infection system that is being studied, but such data are rarely available.

A possible solution for this problem could be to establish/use general links between certain biological traits and contact and transmission patterns [7]. The shape of the transmission–density function is determined by a combination of infection and host characteristics, so based on these characteristics, it should theoretically be possible to *a priori* predict the shape of the function, at least roughly. Knowledge of density-dependent changes in home range size and overlap could, for example, be a useful proxy for the contact–density function. For male brushtail possums (*Trichosurus vulpecula*), it has been established that contacts increase with density according to a positive power function [44], which fits with the fact that this species is not territorial, and with the observation that home ranges are larger at low densities which may result in the maintenance of contacts. Such an inverse correlation between home range size and density was also observed for *M. natalensis* [47], and this may have similar results on contact rates at low densities, as the maintenance of contacts even at very low densities was also observed for this species [26]. This pattern would be expected to be different for territorial species. In an enclosure experiment, movements of meadow voles (*Microtus pennsylvanicus*), which are strongly territorial, decrease significantly with density [48], and although the effect of density on contacts was not measured, it is not unlikely that this decrease in movement distance corresponds with a contact–density function that does not increase, or at least not linearly. As a final example, consider the experimental study of the transmission of the parasitic mite *Coccipolipus hippodamiae* in populations of the two-spot ladybird (*Adalia bipunctata*) [20]. The mite is transmitted sexually, and although sexual contacts are typically assumed to be frequency-dependent, the authors observed that the transmission–density function was closer to linear density-dependence and therefore concluded that the common assumption that sexual transmission is frequency-dependent is not always true. Their study species (*A. bipunctata*), however, is known to be highly promiscuous, which means that sexual contacts are not limited to one or a few mates, but instead increase with density. *A priori* use of this knowledge about host and infection biology would have resulted in the more accurate prediction that sexual transmission of *C. hippodamiae* is density- rather than frequency-dependent.

We would like to note that the patterns observed in this modelling study may change with different transmission characteristics. A longer latent period, for example, might increase invasion and persistence probabilities. Likewise, if immunity is not lifelong, but individuals can instead return to the susceptible class, the infection might persist for longer periods. While such changes might cause the differences between contact–density functions to be more or less outspoken, we doubt that they would change the key patterns observed in this study.

Many wildlife species experience seasonal birth pulses and density fluctuations, and while it has been established that birth pulses can have strong effects on disease transmission [37], we now see that the shape of the transmission–density function can have further significant effects on disease invasion and persistence. The implementation of the transmission–density function should therefore be done with care, and as informed as possible. Although currently few studies have quantified the relationship between contacts and density, other relevant knowledge about host biology and behaviour can potentially be used for deciding on the best possible shape of the transmission–density function.

References

1. Anderson RM, May RM. 1985 Vaccination and herd immunity to infectious diseases. *Nature* **318**, 323–329. (doi:10.1038/318323a0)

2. Bartlett MS. 1957 Measles periodicity and community size. *J. R. Stat. Soc. Ser. A* **120**, 48–70. (doi:10.2307/2342553)

3. Lloyd-Smith JO, Cross PC, Briggs CJ, Daugherty M, Getz WM, Latto J, Sanchez MS, Smith AB, Swei A. 2005 Should we expect population thresholds for

wildlife disease? *Trends Ecol. Evol.* **20**, 511–519. (doi:10.1016/j.tree.2005.07.004)

4. Begon M, Bennett M, Bowers RG, French NP, Hazel SM, Turner J. 2002 A clarification of transmission terms in host-microparasite models: numbers, densities and areas. *Epidemiol. Infect.* **129**, 147–153. (doi:10.1017/s0950268802 007148)

5. Lloyd-Smith JO, Getz WM, Westerhoff H. 2004 Frequency-dependent incidence in models of sexually transmitted diseases: portrayal of pair-based transmission and effects of illness on contact behaviour. *Proc. R. Soc. Lond. B* **271**, 625–634. (doi:10.1098/rspb.2003.2632)

6. Van Boven M, Koopmans M, Van Beest Holle MDR, Meijer A, Klinkenberg D, Donnelly CA, Heesterbeek H. 2007 Detecting emerging transmissibility of avian influenza virus in human households. *PLoS Comput. Biol.* **3**, 1394–1402. (doi:10.1371/journal. pcbi.0030145)

7. Fenton A, Fairbairn JP, Norman R, Hudson PJ. 2002 Parasite transmission: reconciling theory and reality. *J. Anim. Ecol.* **71**, 893–905. (doi:10.1046/ j.1365-2656.2002.00656.x)

8. Anderson RM, May RM. 1979 Population biology of infectious diseases: Part I. *Nature* **280**, 361–367. (doi:10.1038/280361a0)

9. Heesterbeek J. 2002 A brief history of R_0 and a recipe for its calculation. *Acta Biotheor.* **50**, 189–204. (doi:10.1023/A:1016599411804)

10. McCallum H, Barlow N, Hone J. 2001 How should pathogen transmission be modelled? *Trends Ecol. Evol.* **16**, 295–300. (doi:10.1016/s0169-5347(01) 02144-9)

11. de Jong MCM, Diekmann O, Heesterbeek H. 1995 How does transmission of infection depend on population size? *Publ. Newt. Inst.* **5**, 84–94.

12. Getz W, Pickering J. 1983 Epidemic models: thresholds and population regulation. *Am. Nat.* **121**, 892–898. (doi:10.1086/284112)

13. Keeling MJ, Rohani P. 2008 *Modeling infectious diseases in humans and animals.* Princeton, NJ: Princeton University Press.

14. Bjørnstad ON, Finkenstädt BF, Grenfell BT. 2002 Dynamics of measles epidemics: estimating scaling of transmission rates using a time series SIR model. *Ecol. Monogr.* **72**, 169–184. (doi:10.1890/0012-9615 (2002)072[0169:DOMEES]2.0.CO;2)

15. Smith MJ, Telfer S, Kallio ER, Burthe S, Cook AR, Lambin X, Begon M. 2009 Host-pathogen time series data in wildlife support a transmission function between density and frequency dependence. *Proc. Natl Acad. Sci. USA* **106**, 7905–7909. (doi:10.1073/pnas.0809 145106)

16. Ryder JJ, Miller MR, White A, Knell RJ, Boots M. 2007 Host-parasite population dynamics under combined frequency- and density-dependent transmission. *Oikos* **116**, 2017–2026. (doi:10.1111/j. 2007.0030-1299.15863.x)

17. Knell RJ, Begon M, Thompson DJ. 1996 Transmission dynamics of *Bacillus thuringiensis* infecting *Plodia interpunctella*: a test of the mass action assumption with an insect pathogen. *Proc. R. Soc. Lond. B* **263**, 75–81. (doi:10.1098/rspb.1996.0013)

18. Rachowicz LJ, Briggs CJ. 2007 Quantifying the disease transmission function: effects of density on *Batrachochytrium dendrobatidis* transmission in the mountain yellow-legged frog *Rana muscosa*. *J.*

Anim. Ecol. **76**, 711–721. (doi:10.1111/j.1365-2656. 2007.01256.x)

19. Goyens J, Reijniers J, Borremans B, Leirs H. 2013 Density thresholds for Mopeia virus invasion and persistence in its host *Mastomys natalensis*. *J. Theor. Biol.* **317**, 55–61. (doi:10.1016/j.jtbi.2012. 09.039)

20. Ryder JJ, Webberley KM, Boots M, Knell RJ. 2005 Measuring the transmission dynamics of a sexually transmitted disease. *Proc. Natl Acad. Sci. USA* **102**, 15 140–15 143. (doi:10.1073/pnas.0505139102)

21. Luis AD, Douglass RJD, Mills JNM, Bjørnstad ON. 2015 Environmental fluctuations lead to predictability in Sin Nombre hantavirus outbreaks. *Ecology* **96**, 1691–1701. (doi:10.1890/14-1910.1)

22. Greer AL, Briggs CJ, Collins JP. 2008 Testing a key assumption of host-pathogen theory: density and disease transmission. *Oikos* **117**, 1667–1673. (doi:10.1111/j.1600-0706.2008.16783.x)

23. Heesterbeek JA, Metz JA. 1993 The saturating contact rate in marriage- and epidemic models. *J. Math. Biol.* **31**, 529–539. (doi:10.1007/bf00173891)

24. Hu H, Nigmatulina K, Eckhoff P. 2013 The scaling of contact rates with population density for the infectious disease models. *Math. Biosci.* **244**, 125–134. (doi:10.1016/j.mbs.2013.04.013)

25. McCallum H *et al.* 2017 Breaking beta: deconstructing the parasite transmission function. *Phil. Trans. R. Soc. B* **372**, 20160084. (doi:10.1098/ rstb.2016.0084)

26. Borremans B, Reijniers J, Hughes NK, Godfrey SS, Gryseels S, Makundi R, Leirs H. 2017 Nonlinear scaling of foraging contacts with rodent population density. *Oikos* **126**, 792–800. (doi:10.1111/oik.03623)

27. Borremans B, Vossen R, Becker-Ziaja B, Gryseels S, Hughes N, Van Gestel M, Van Houtte N, Günther S, Leirs H. 2015 Shedding dynamics of Morogoro virus, an African arenavirus closely related to Lassa virus, in its natural reservoir host *Mastomys natalensis*. *Sci. Rep.* **5**, 10445. (doi:10.1038/srep10445)

28. Katakweba A, Mulungu L, Eiseb S, Mahlaba T, Makundi R, Massawe A, Borremans B, Belmain S. 2012 Prevalence of haemoparasites, leptospires and coccobacilli with potential for human infection in the blood of rodents and shrews from selected localities in Tanzania, Namibia and Swaziland. *Afr. Zool.* **47**, 119–127. (doi:10.3377/004.047.0112)

29. Frame JD, Baldwin JM, Gocke DJ, Troup JM. 1970 Lassa fever, a new virus disease of man from West Africa. 1. Clinical description and pathological findings. *Am. J. Trop. Med. Hyg.* **19**, 670–676. (doi:10.4269/ajtmh.1970.19.670)

30. Davis DH. 1953 Plague in Africa from 1935 to 1949; a survey of wild rodents in African territories. *Bull. World Health Organ.* **9**, 665–700.

31. Gryseels S, Rieger T, Oestereich L, Cuypers B, Borremans B, Makundi R, Leirs H, Günther S, Goüy de Bellocq J. 2015 Gairo virus, a novel arenavirus of the widespread *Mastomys natalensis*: genetically divergent, but ecologically similar to Lassa and Morogoro viruses. *Virology* **476**, 249–256. (doi:10.1016/j.virol.2014.12.011)

32. Goüy de Bellocq J, Borremans B, Katakweba A, Makundi R, Baird SJE, Becker-Ziaja B, Günther S, Leirs H. 2010 Sympatric occurrence of 3 Arenaviruses, Tanzania. *Emerg. Infect. Dis.* **16**, 10–13. (doi:10.3201/eid1604.091721)

33. Leirs H, Stenseth NC, Nichols JD, Hines JE, Verhagen R, Verheyen W. 1997 Stochastic seasonality and

nonlinear density-dependent factors regulate population size in an African rodent. *Nature* **389**, 176–180. (doi:10.1038/38271)

34. Sluydts V, Davis S, Mercelis S, Leirs H. 2009 Comparison of multimammate mouse (*Mastomys natalensis*) demography in monoculture and mosaic agricultural habitat: implications for pest management. *Crop Prot.* **28**, 647–654. (doi:10.10 16/j.cropro.2009.03.018)

35. Borremans B, Leirs H, Gryseels S, Günther S, Makundi R, Goüy de Bellocq J. 2011 Presence of Mopeia virus, an African arenavirus, related to biotope and individual rodent host characteristics: implications for virus transmission. *Vector-Borne Zoonotic Dis.* **11**, 1125–1131. (doi:10.1089/vbz.2010. 0010)

36. Mariën J, Borremans B, Gryseels S, Broecke BV, Becker-Ziaja B, Makundi R, Massawe A, Reijniers J, Leirs H. 2017 Arenavirus dynamics in experimentally and naturally infected rodents. *Ecohealth* **14**, 463–473. (doi:10.1007/s10393-017-1256-7)

37. Peel AJ, Pulliam JRC, Luis AD, Plowright RK, Shea TJO, Hayman DTS, Wood JLN, Webb CT, Restif O. 2014 The effect of seasonal birth pulses on pathogen persistence in wild mammal populations. *Proc. R. Soc. B* **281**, 20132962. (doi:10.1098/rspb.2013. 2962)

38. Ross R. 1916 An application of the theory of probabilities to the study of a priori pathometry: part I. *Proc. R. Soc. Lond. A* **92**, 204–230. (doi:10.1098/rspa.1916.0007)

39. Kermack WO, McKendrick AG. 1927 A contribution to the mathematical theory of epidemics. *Proc. R. Soc. Lond. Ser. A* **115**, 700–721. (doi:10.1098/rspa.1927. 0118)

40. Cao Y, Gillespie DT, Petzold LR. 2007 Adaptive explicit-implicit tau-leaping method with automatic tau selection. *J. Chem. Phys.* **126**, 224101. (doi:10.1063/1.2745299)

41. Thrall PH, Antonovics J, Hall DW. 1993 Host and pathogen coexistence in sexually transmitted and vector-borne diseases characterized by frequency-dependent disease transmission. *Am. Nat.* **142**, 543–552. (doi:10.1086/285554)

42. de Jong MCMM, Bouma A, Diekmann O, Heesterbeek H. 2002 Modelling transmission: mass action and beyond. *Trends Ecol. Evol.* **17**, 5347. (doi:10.1016/S0169-5347(01)02398-9)

43. Vander Wal E, Yip H, McLoughlin PD. 2012 Sex-based differences in density-dependent sociality: an experiment with a gregarious ungulate. *Ecology* **93**, 206–212. (doi:10.1890/11-0020.1)

44. Ramsey D, Spencer N, Caley P, Efford M, Hansen K, Lam M, Cooper D. 2002 The effects of reducing population density on contact rates between brushtail possums: implications for transmission of bovine tuberculosis. *J. Appl. Ecol.* **39**, 806–818. (doi:10.1046/j.1365-2664.2002. 00760.x)

45. Cross P, Creech T, Ebinger M, Manlove K. 2013 Female elk contacts are neither frequency nor density dependent. *Ecology* **94**, 2076–2086. (doi:10.1890/12-2086.1)

46. Borremans B, Reijniers J, Hughes NK, Godfrey SS, Gryseels S, Makundi R, Leirs H. 2017 Data from: Nonlinear scaling of foraging contacts with rodent population density. Dryad Digital Repository. (http://dx.doi.org/10.5061/dryad. 92tn2)

47. Borremans B, Hughes NK, Reijniers J, Sluydts V, Katakweba AAS, Mulungu LS, Sabuni CA, Makundi RH, Leirs H. 2014 Happily together forever: temporal variation in spatial patterns and complete lack of territoriality in a promiscuous rodent. *Popul. Ecol.* **56**, 109–118. (doi:10.1007/s10144-013-0393-2)

48. Ostfeld RS, Canham CD. 1995 Density-dependent processes in meadow voles: an experimental approach. *Ecology* **76**, 521–532. (doi:10.2307/1941210)